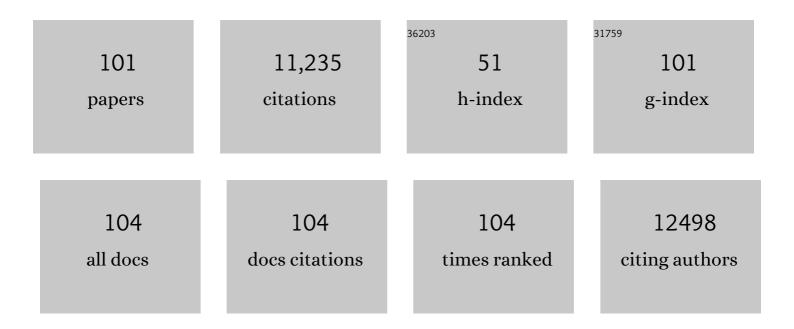
List of Publications by Year in descending order

Source: https://exaly.com/author-pdf/3966283/publications.pdf Version: 2024-02-01



#	Article	IF	CITATIONS
1	Carbon Defects Induced Delocalization of π Electrons Enables Efficient Charge Separation in Graphitic Carbon Nitride for Increased Photocatalytic H2 Generation. Catalysis Letters, 2022, 152, 669-678.	1.4	6
2	Microwave awakening the n-ï€* electronic transition in highly crystalline polymeric carbon nitride nanosheets for photocatalytic hydrogen generation. Journal of Energy Chemistry, 2022, 65, 541-547.	7.1	48
3	Revealing dual roles of g-C3N4 in Chlorella vulgaris cultivation. Journal of Hazardous Materials, 2022, 424, 127639.	6.5	10
4	Three-dimensional surface-enhanced Raman scattering substrates constructed by integrating template-assisted electrodeposition and post-growth of silver nanoparticles. Journal of Colloid and Interface Science, 2022, 608, 2111-2119.	5.0	13
5	A composite consisting of intermetallic Ni3Fe and nitrogen-doped carbon for electrocatalytic water oxidation: The effect of increased pyridinic nitrogen dopant. Ceramics International, 2022, 48, 5759-5765.	2.3	4
6	CdS/Bi12O17Cl2 Heterostructure Promotes Visible-Light-Driven Photocatalytic CH4 Generation and Phenol Conversion. International Journal of Photoenergy, 2022, 2022, 1-12.	1.4	2
7	Highly soluble Ni-salen molecules enable boosted photocatalytic hydrogen evolution of polymeric carbon nitride/CdS heterojunction. Journal of Alloys and Compounds, 2022, 915, 165351.	2.8	6
8	Understanding the photothermal contribution to electrocatalysis: A case study of carbon supported NiFe layered double hydroxide. International Journal of Hydrogen Energy, 2022, 47, 23971-23979.	3.8	8
9	Engineering graphitic carbon nitride with expanded interlayer distance for boosting photocatalytic hydrogen evolution. Chinese Journal of Catalysis, 2021, 42, 217-224.	6.9	31
10	Increasing π-electron availability in benzene ring incorporated graphitic carbon nitride for increased photocatalytic hydrogen generation. Journal of Materials Science and Technology, 2021, 65, 164-170.	5.6	26
11	Atomic-level localization of π-electrons in defect engineered tri- <i>s</i> -triazine units for increased photocatalytic hydrogen generation of polymeric carbon nitride. Catalysis Science and Technology, 2021, 11, 5663-5670.	2.1	9
12	Unravelling intramolecular charge transfer in donor–acceptor structured g-C ₃ N ₄ for superior photocatalytic hydrogen evolution. Journal of Materials Chemistry A, 2021, 9, 1207-1212.	5.2	40
13	Surface plasmons activate the oxygen evolution reaction over nickel hydroxide electrocatalysts. International Journal of Hydrogen Energy, 2021, 46, 21433-21441.	3.8	9
14	Molecular Engineering to Tune the Ligand Environment of Atomically Dispersed Nickel for Efficient Alcohol Electrochemical Oxidation. Advanced Functional Materials, 2021, 31, 2106349.	7.8	27
15	Facile steam activation route to synthesize S-doped graphitic polymeric carbon nitride nanosheets for increased photocatalytic H2 generation. Materials Letters, 2021, 300, 130120.	1.3	3
16	Up-cycling of waste paper for increased photo-catalytic hydrogen generation of graphitic carbon nitride under visible light exposure. Journal of the Taiwan Institute of Chemical Engineers, 2021, 127, 259-264.	2.7	0
17	Ascorbic acid-assisted hydrothermal route to create mesopores in polymeric carbon nitride for increased photocatalytic hydrogen generation. International Journal of Hydrogen Energy, 2021, 46, 38310-38318.	3.8	14
18	Bio-removal of PtCl62â^' complex by Galdieria sulphuraria. Science of the Total Environment, 2021, 796, 149021.	3.9	16

#	Article	IF	CITATIONS
19	Facile one-step "polymerization-exfoliation―route to crystalline graphitic carbon nitride nanosheets for increased photocatalytic hydrogen evolution. Applied Surface Science, 2020, 501, 144259.	3.1	18
20	Lowering the schottky barrier of g-C3N4/Carbon graphite heterostructure by N-doping for increased photocatalytic hydrogen generation. Applied Catalysis B: Environmental, 2020, 278, 119253.	10.8	66
21	Understanding the Enhanced Electrocatalytic Hydrogen Evolution <i>via</i> Integrating Electrochemically Inactive g-C ₃ N ₄ : The Effect of Interfacial Engineering. ACS Sustainable Chemistry and Engineering, 2020, 8, 10313-10320.	3.2	28
22	Awakening nÂ→Âï€* electronic transition by breaking hydrogen bonds in graphitic carbon nitride for increased photocatalytic hydrogen generation. Chemical Engineering Journal, 2020, 399, 125847.	6.6	36
23	Control of Nitrogen Vacancy in g-C ₃ N ₄ by Heat Treatment in an Ammonia Atmosphere for Enhanced Photocatalytic Hydrogen Generation. Wuli Huaxue Xuebao/ Acta Physico - Chimica Sinica, 2020, 36, 1905056-0.	2.2	18
24	Achieving Efficient Incorporation of Ï€â€Electrons into Graphitic Carbon Nitride for Markedly Improved Hydrogen Generation. Angewandte Chemie, 2019, 131, 2007-2011.	1.6	51
25	Protonation and microwave-assisted heating induced excitation of lone-pair electrons in graphitic carbon nitride for increased photocatalytic hydrogen generation. Journal of Materials Chemistry A, 2019, 7, 20223-20228.	5.2	56
26	UiO-66 MOFs as electron transport channel to short circuit dye photosensitizer and NiS2 co-catalyst for increased hydrogen generation. Materials Letters, 2019, 255, 126593.	1.3	9
27	Rücktitelbild: Achieving Efficient Incorporation of π-Electrons into Graphitic Carbon Nitride for Markedly Improved Hydrogen Generation (Angew. Chem. 7/2019). Angewandte Chemie, 2019, 131, 2178-2178.	1.6	2
28	A surface carbonization strategy towards MoS ₂ microspheres with enhanced electrochemical hydrogen evolution activity. New Journal of Chemistry, 2019, 43, 9583-9588.	1.4	6
29	Maximizing the photocatalytic hydrogen evolution of Z-scheme UiO-66-NH2@Au@CdS by aminated-functionalized linkers. Journal of Materials Science: Materials in Electronics, 2019, 30, 5203-5211.	1.1	9
30	Ultrafine 1D graphene interlayer in g-C3N4/graphene/recycled carbon fiber heterostructure for enhanced photocatalytic hydrogen generation. Chemical Engineering Journal, 2019, 359, 1352-1359.	6.6	46
31	Achieving Efficient Incorporation of Ï€â€Electrons into Graphitic Carbon Nitride for Markedly Improved Hydrogen Generation. Angewandte Chemie - International Edition, 2019, 58, 1985-1989.	7.2	199
32	A microwave-assisted thermolysis route to single-step preparation of MoS ₂ /CdS composite photocatalysts for active hydrogen generation. Sustainable Energy and Fuels, 2018, 2, 430-435.	2.5	27
33	Hybrid NiO–CuO mesoporous nanowire array with abundant oxygen vacancies and a hollow structure as a high-performance asymmetric supercapacitor. Journal of Materials Chemistry A, 2018, 6, 21131-21142.	5.2	132
34	MOFs as an electron-transfer-bridge between a dye photosensitizer and a low cost Ni ₂ P co-catalyst for increased photocatalytic H ₂ generation. Sustainable Energy and Fuels, 2018, 2, 2502-2506.	2.5	19
35	A highly stable non-noble metal Ni ₂ P co-catalyst for increased H ₂ generation by g-C ₃ N ₄ under visible light irradiation. Journal of Materials Chemistry A, 2017, 5, 8493-8498.	5.2	190
36	A general and rapid approach to crystalline metal sulfide nanoparticle synthesis for photocatalytic H ₂ generation. Journal of Materials Chemistry A, 2017, 5, 21669-21673.	5.2	17

#	Article	IF	CITATIONS
37	Ni(dmgH) 2 complex coupled with metal-organic frameworks MIL-101(Cr) for photocatalytic H 2 evolution under visible light irradiation. Journal of Materiomics, 2017, 3, 58-62.	2.8	24
38	Bandgap engineering of ternary sulfide nanocrystals by solution proton alloying for efficient photocatalytic H2 evolution. Nano Energy, 2016, 26, 577-585.	8.2	23
39	A Rapid Microwaveâ€Assisted Thermolysis Route to Highly Crystalline Carbon Nitrides for Efficient Hydrogen Generation. Angewandte Chemie, 2016, 128, 14913-14917.	1.6	234
40	A Rapid Microwaveâ€Assisted Thermolysis Route to Highly Crystalline Carbon Nitrides for Efficient Hydrogen Generation. Angewandte Chemie - International Edition, 2016, 55, 14693-14697.	7.2	335
41	Synthesis of TiO ₂ /rGO Nanocomposites with Enhanced Photoelectrochemical Performance and Photocatalytic Activity. Nano, 2016, 11, 1650007.	0.5	9
42	Dye-sensitized MIL-101 metal organic frameworks loaded with Ni/NiO _x nanoparticles for efficient visible-light-driven hydrogen generation. APL Materials, 2015, 3, 104403.	2.2	59
43	Improving the photocatalytic performance of polyimide by constructing an inorganic-organic hybrid ZnO-polyimide core–shell structure. Journal of Molecular Catalysis A, 2015, 406, 46-50.	4.8	49
44	MoP is a novel, noble-metal-free cocatalyst for enhanced photocatalytic hydrogen production from water under visible light. Journal of Materials Chemistry A, 2015, 3, 16941-16947.	5.2	211
45	Rapid microwave-assisted green production of a crystalline polyimide for enhanced visible-light-induced photocatalytic hydrogen production. Journal of Materials Chemistry A, 2015, 3, 10205-10208.	5.2	64
46	In situ growth of CdS nanoparticles on UiO-66 metal-organic framework octahedrons for enhanced photocatalytic hydrogen production under visible light irradiation. Applied Surface Science, 2015, 346, 278-283.	3.1	197
47	Approximate microwave heating models for global temperature profile in rectangular medium with TE10 mode. Journal of Thermal Analysis and Calorimetry, 2015, 122, 487-495.	2.0	9
48	Quasiâ€Polymeric Metal–Organic Framework UiOâ€66/gâ€C ₃ N ₄ Heterojunctions for Enhanced Photocatalytic Hydrogen Evolution under Visible Light Irradiation. Advanced Materials Interfaces, 2015, 2, 1500037.	1.9	260
49	A review on g-C3N4 for photocatalytic water splitting and CO2 reduction. Applied Surface Science, 2015, 358, 15-27.	3.1	684
50	Improving photocatalytic hydrogen production of metal–organic framework UiO-66 octahedrons by dye-sensitization. Applied Catalysis B: Environmental, 2015, 168-169, 572-576.	10.8	252
51	Microwave-assisted heating synthesis: a general and rapid strategy for large-scale production of highly crystalline g-C ₃ N ₄ with enhanced photocatalytic H ₂ production. Green Chemistry, 2014, 16, 4663-4668.	4.6	166
52	Magnetic Fe3O4@C/Cu and Fe3O4@CuO core–shell composites constructed from MOF-based materials and their photocatalytic properties under visible light. Applied Catalysis B: Environmental, 2014, 144, 863-869.	10.8	153
53	Solar-to-fuels conversion over In2O3/g-C3N4 hybrid photocatalysts. Applied Catalysis B: Environmental, 2014, 147, 940-946.	10.8	398
54	Noble-metal-free g-C3N4/Ni(dmgH)2 composite for efficient photocatalytic hydrogen evolution under visible light irradiation. Applied Surface Science, 2014, 319, 344-349.	3.1	169

#	Article	IF	CITATIONS
55	Metal–organic frameworks MIL-88A hexagonal microrods as a new photocatalyst for efficient decolorization of methylene blue dye. Dalton Transactions, 2014, 43, 3792-3798.	1.6	231
56	Inorganic–organic hybrid NiO–g-C ₃ N ₄ photocatalyst for efficient methylene blue degradation using visible light. RSC Advances, 2014, 4, 22491-22496.	1.7	70
57	Fabrication of magnetically separable fluorescent terbium-based MOF nanospheres for highly selective trace-level detection of TNT. Dalton Transactions, 2014, 43, 3978.	1.6	83
58	Enhanced visible-light-driven photocatalytic hydrogen generation over g-C3N4 through loading the noble metal-free NiS2 cocatalyst. RSC Advances, 2014, 4, 6127.	1.7	136
59	Hetero-nanostructured suspended photocatalysts for solar-to-fuel conversion. Energy and Environmental Science, 2014, 7, 3934-3951.	15.6	470
60	Efficient CO ₂ Capture and Photoreduction by Amineâ€Functionalized TiO ₂ . Chemistry - A European Journal, 2014, 20, 10220-10222.	1.7	95
61	Controllable synthesis of Mg–Fe layered double hydroxide nanoplates with specific Mg/Fe ratios and their effect on adsorption of As(<scp>v</scp>) from water. New Journal of Chemistry, 2014, 38, 4427.	1.4	28
62	The elastic behavior of dense C3N4 under high pressure: First-principles calculations. Journal of Physics and Chemistry of Solids, 2014, 75, 1324-1333.	1.9	13
63	Porous Fe3O4/CuI/PANI nanosheets with excellent microwave absorption and hydrophobic property. Materials Research Bulletin, 2014, 53, 58-64.	2.7	30
64	One-pot synthesis of novel Fe3O4/Cu2O/PANI nanocomposites as absorbents in water treatment. Journal of Materials Chemistry A, 2014, 2, 7953.	5.2	51
65	First principles calculations of the pressure affection to g-C3N4. Computational Materials Science, 2014, 91, 258-265.	1.4	16
66	Au@TiO ₂ –CdS Ternary Nanostructures for Efficient Visible-Light-Driven Hydrogen Generation. ACS Applied Materials & Interfaces, 2013, 5, 8088-8092.	4.0	177
67	An easy method to synthesize graphene oxide–FeOOH composites and their potential application in water purification. Materials Research Bulletin, 2013, 48, 2180-2185.	2.7	51
68	Artificial photosynthetic hydrogen evolution over g-C3N4 nanosheets coupled with cobaloxime. Physical Chemistry Chemical Physics, 2013, 15, 18363.	1.3	101
69	A novel magnetic recyclable photocatalyst based on a core–shell metal–organic framework Fe3O4@MIL-100(Fe) for the decolorization of methylene blue dye. Journal of Materials Chemistry A, 2013, 1, 14329.	5.2	375
70	Large impact of heating time on physical properties and photocatalytic H2 production of g-C3N4 nanosheets synthesized through urea polymerization in Ar atmosphere. International Journal of Hydrogen Energy, 2013, 38, 13159-13163.	3.8	103
71	In-situ growth of CdS quantum dots on g-C3N4 nanosheets for highly efficient photocatalytic hydrogen generation under visible light irradiation. International Journal of Hydrogen Energy, 2013, 38, 1258-1266.	3.8	339
72	Facile fabrication of magnetically separable graphitic carbon nitride photocatalysts with enhanced photocatalytic activity under visible light. Journal of Materials Chemistry A, 2013, 1, 3008.	5.2	216

#	Article	IF	CITATIONS
73	NiS2 Co-catalyst decoration on CdLa2S4 nanocrystals for efficient photocatalytic hydrogen generation under visible light irradiation. International Journal of Hydrogen Energy, 2013, 38, 7218-7223.	3.8	76
74	Red phosphor/g-C3N4 heterojunction with enhanced photocatalytic activities for solar fuels production. Applied Catalysis B: Environmental, 2013, 140-141, 164-168.	10.8	219
75	Rapid synthesis of nanoscale terbium-based metal–organic frameworks by a combined ultrasound-vapour phase diffusion method for highly selective sensing of picric acid. Journal of Materials Chemistry A, 2013, 1, 8745.	5.2	182
76	Ultrafast microwave-enhanced ionothermal synthesis of luminescent crystalline polyimide nanosheets for highly selective sensing of chromium ions. Inorganic Chemistry Communication, 2013, 29, 128-130.	1.8	20
77	Hierarchically mesostructured MIL-101 metal–organic frameworks: supramolecular template-directed synthesis and accelerated adsorption kinetics for dye removal. CrystEngComm, 2012, 14, 1613-1617.	1.3	169
78	Fabrication of composite photocatalyst g-C3N4–ZnO and enhancement of photocatalytic activity under visible light. Dalton Transactions, 2012, 41, 6756.	1.6	553
79	Fe3O4@MOF core–shell magnetic microspheres with a designable metal–organic framework shell. Journal of Materials Chemistry, 2012, 22, 9497.	6.7	285
80	A Rational Self‧acrificing Template Route to Metal–Organic Framework Nanotubes and Reversible Vaporâ€Phase Detection of Nitroaromatic Explosives. Small, 2012, 8, 225-230.	5.2	99
81	Facile synthesis of highly luminescent nanowires of a terbium-based metal–organic framework by an ultrasonic-assisted method and their application as a luminescent probe for selective sensing of organoamines. Inorganic Chemistry Communication, 2012, 17, 147-150.	1.8	49
82	Microwave-assisted synthesis of highly fluorescent nanoparticles of a melamine-based porous covalent organic framework for trace-level detection of nitroaromatic explosives. Journal of Hazardous Materials, 2012, 221-222, 147-154.	6.5	145
83	Facile fabrication of magnetic metal–organic framework nanocomposites for potential targeted drug delivery. Journal of Materials Chemistry, 2011, 21, 3843.	6.7	343
84	Thiol-functionalization of metal-organic framework by a facile coordination-based postsynthetic strategy and enhanced removal of Hg2+ from water. Journal of Hazardous Materials, 2011, 196, 36-43.	6.5	456
85	Surfactant-assisted facile synthesis of fluorescent zinc benzenedicarboxylate metal-organic framework nanorods with enhanced nitrobenzene explosives detection. Materials Chemistry and Physics, 2011, 131, 358-361.	2.0	43
86	Influence of the crystallinity of the iron catalysts on the formation of carbon nanotubes. Materials Research Bulletin, 2011, 46, 884-887.	2.7	4
87	Surfactant-assisted synthesis of lanthanide metal-organic framework nanorods and their fluorescence sensing of nitroaromatic explosives. Materials Letters, 2011, 65, 1385-1387.	1.3	68
88	Microwave-enhanced synthesis of magnetic porous covalent triazine-based framework composites for fast separation of organic dye from aqueous solution. Journal of Hazardous Materials, 2011, 186, 984-990.	6.5	137
89	New photocatalysts based on MIL-53 metal–organic frameworks for the decolorization of methylene blue dye. Journal of Hazardous Materials, 2011, 190, 945-951.	6.5	416
90	Facile Method To Synthesize Mesoporous Multimetal Oxides (ATiO ₃ , A = Sr, Ba) with Large Specific Surface Areas and Crystalline Pore walls. Chemistry of Materials, 2010, 22, 1276-1278.	3.2	45

#	Article	IF	CITATIONS
91	Highly energy- and time-efficient synthesis of porous triazine-based framework: microwave-enhanced ionothermal polymerization and hydrogen uptake. Journal of Materials Chemistry, 2010, 20, 6413.	6.7	99
92	Polymerizable complex synthesis of BaZr1â^'xSnxO3 photocatalysts: Role of Sn4+ in the band structure and their photocatalytic water splitting activities. Journal of Materials Chemistry, 2010, 20, 6772.	6.7	52
93	NaNbO3 Nanostructures: Facile Synthesis, Characterization, and Their Photocatalytic Properties. Catalysis Letters, 2009, 132, 205-212.	1.4	96
94	Visible-Light-Induced Photocatalytic Oxidation of Polycyclic Aromatic Hydrocarbons over Tantalum Oxynitride Photocatalysts. Environmental Science & Technology, 2009, 43, 2919-2924.	4.6	96
95	BaCeO3 as a novel photocatalyst with 4f electronic configuration for water splitting. Solid State lonics, 2008, 178, 1711-1713.	1.3	38
96	Synthesis and photocatalytic characterization of a new photocatalyst BaZrO3. International Journal of Hydrogen Energy, 2008, 33, 5941-5946.	3.8	130
97	Enhanced Photocatalytic Water Splitting Properties of KNbO ₃ Nanowires Synthesized through Hydrothermal Method. Journal of Physical Chemistry C, 2008, 112, 18846-18848.	1.5	135
98	Efficient Photodegradation of Phenanthrene under Visible Light Irradiation via Photosensitized Electron Transfer. Journal of Physical Chemistry C, 2008, 112, 4291-4296.	1.5	21
99	Large impact of strontium substitution on photocatalytic water splitting activity of BaSnO3. Applied Physics Letters, 2007, 91, .	1.5	74
100	Synthesis and characterization of Sr- and Mg-doped LaGaO3 by using glycine–nitrate combustion method. Journal of Alloys and Compounds, 2006, 425, 348-352.	2.8	41
101	Microstructure and mechanical properties of ultrafine Ti(CN)-based cermets fabricated from nano/submicron starting powders. Ceramics International, 2005, 31, 851-862.	2.3	59